

https://doi.org/10.1070/QEL16794

Generation of narrow-band single-photon states via spontaneous parametric down-conversion for quantum memories in doped crystals

D.O. Akat'ev, I.Z. Latypov, A.V. Shkalikov, A.A. Kalachev

Abstract. **We present experimental results on the generation of narrow-band single-photon states via cavity-enhanced spontaneous parametric down-conversion in a PPLN crystal and demonstrate the feasibility of conditional preparation of single 867-nm photons with a 70-MHz linewidth, compatible with optical quantum memory devices based on Nd^{3+}-doped isotopically pure Y^7LiF_4 crystals.**

Keywords: *single-photon source, spontaneous parametric down-conversion, cavity.*

1. Introduction

Single-photon states of an electromagnetic field are important for many applications in quantum optics and quantum information science, such as optical quantum computing, random number generation, metrology and quantum communications [1–4], so a topical issue in quantum optical technologies is to develop sources of single-photon states of light [5–7]. In an ideal case, such a source should be deterministic, i.e. it should produce single photons on demand. However, in many practically important cases, it is sufficient to have nondeterministic, heralded photon sources [8], which can be ensured e.g. with the use of spontaneous parametric down-conversion (SPDC) of light [9, 10]. Distinctive features of SPDC include a broad emission spectrum, up to several terahertz, and two-photon correlations in scattered field modes. As a result, SPDC-based sources allow for the generation of pure single-photon states and various entangled two-photon states in wide wavelength and duration ranges at room temperature [5, 8]. It is important to note that sources of narrow-band single-photon states are necessary to implement quantum communication and quantum computing protocols requiring the use of optical quantum memories. For example, to ensure effective recording of single-photon pulses in ensembles of atoms or ions, the spectral width of light should be from a few to a hundred megahertz. In this context, a promising approach is to use cavity-enhanced SPDC [11], which allows one to reduce the SPDC linewidth to a few megahertz and below, simultaneously raising the spectral brightness of the source (see e.g. Refs [12–20]).

D.O. Akat'ev, I.Z. Latypov, A.V. Shkalikov, A.A. Kalachev
E.K. Zavoisky Physical-Technical Institute, Kazan Scientific Centre, Russian Academy of Sciences, Sibirskii trakt 10/7, 420029 Kazan, Tatarstan, Russia; e-mail: a.a.kalachev@mail.ru

Received 31 July 2018
Kvantovaya Elektronika **48** (10) 902–905 (2018)
Translated by O.M. Tsarev

In this work, we demonstrate a cavity SPDC-based single-photon source compatible with optical quantum memory devices based on rare-earth-doped dielectric crystals. In particular, the proposed source generates narrow-band single-photon states that can be stored and reproduced in a Nd^{3+}-doped isotopically pure Y^7LiF_4 crystal. A distinctive feature of this material is the small inhomogeneous linewidth of optical transitions of dopant ions (70 MHz or smaller), which makes it potentially attractive for solid-state nonresonant optical quantum memories [21].

2. Conditional preparation of single-photon states in a single-resonant optical parametric oscillator

SPDC can be defined as interaction between three electromagnetic field modes in a quadratically nonlinear medium, a process in which disappearance of a photon in one mode (pump mode) is accompanied by the creation of two photons in the other modes (usually referred to as the signal and idler modes). The state vector of a two-photon field (biphoton) can be written as follows [22]:

$$|\Psi\rangle = |0\rangle + \int\int \mathrm{d}\omega_\mathrm{s}\mathrm{d}\omega_\mathrm{i} F(\omega_\mathrm{s},\omega_\mathrm{i})|\omega_\mathrm{s}\rangle|\omega_\mathrm{i}\rangle, \quad (1)$$

where $F(\omega_\mathrm{s},\omega_\mathrm{i})$ is the two-photon spectral amplitude, which determines the spectral and temporal properties of correlated photons, and $|\omega_\mathrm{s}\rangle$ and $|\omega_\mathrm{i}\rangle$ are single-photon states of a mode of frequency ω of the signal (s) and idler (i) fields. In the case of collinear generation in a periodically poled nonlinear medium, the biphoton amplitude can be represented as

$$F(\omega_\mathrm{s},\omega_\mathrm{i}) = |A|^2 \mathrm{sinc}(\Delta kL/2), \quad (2)$$

where $|A|^2$ is the effective interaction coefficient which takes into account the nonlinearity of the medium, mode interaction geometry and other factors [22, 23]; $\Delta k = k_\mathrm{p} - k_\mathrm{i} - k_\mathrm{s} - 2\pi/\Lambda$ is the wave vector mismatch; Λ is the nonlinearity modulation period; $k_m = \omega_m n(\omega_m)/c$ is the wave vector corresponding to the mth mode (m = i, s or p, where p refers to the pump field); and $n(\omega_m)$ is the refractive index.

The operation of an SPDC-based single-photon source is based on the correlation between the numbers of photons in scattered field modes, represented by (1). Detection of one photon in a pair (e.g. the idler photon) unambiguously indicates the presence of the other (signal photon), so such sources are referred to as heralded sources. Since the SPDC field includes contributions from not only the two-photon state (1)

but also multiphoton states, the degree of proximity to the single-photon state of the field at the output is characterised by the magnitude of the normalised second-order autocorrelation function $g^{(2)}(\tau)$ at zero time delay, $\tau = 0$:

$$g^{(2)}(0) = \frac{\langle a^{\dagger 2} a^2 \rangle}{\langle a^\dagger a \rangle^2}, \tag{3}$$

where a is the photon annihilation operator in the spatiotemporal field mode under consideration at the source output. In the case of an ideal single-photon source, we have $g^{(2)}(0) = 0$, which means that there is no contribution from multiphoton states.

One effective approach for implementing a frequency-tunable narrow-band single-photon light source is intracavity SPDC, corresponding to a single-resonant optical parametric oscillator (OPO). In this case, the cavity amplifies only one of the interacting fields (e.g. the signal field), whereas the other two (idler and pump) fields propagate through the cavity mirrors without reflection. Even though not raising the source brightness relative to cavity-free SPDC, such a configuration significantly facilitates experimental implementation because it does not require that the OPO be adjusted to several modes [12]. In such a case, the resonance (signal) photon power spectrum takes the form [24]

$$S(\omega) \propto \sum_{j=-\infty}^{\infty} \frac{\mathrm{sinc}^2(j\Delta\omega_{\mathrm{FSR}}\tau_0/2)}{(\Delta\omega_{\mathrm{mod}}/2)^2 + (\omega_{\mathrm{s}} - j\Delta\omega_{\mathrm{FSR}} - \omega)^2}, \tag{4}$$

where τ_0 is the difference between the times needed for the signal and idler photons to traverse the crystal; $\Delta\omega_{\mathrm{FSR}}$ is the free spectral range of the OPO; and $\Delta\omega_{\mathrm{mod}}$ is the cavity mode width. In this formula, the numerator represents the spectral density envelope with no cavity, and the denominator represents enhanced generation of photon pairs in which one photon corresponds to cavity eigenmodes at frequencies $\omega_{\mathrm{s}} - j\Delta\omega_{\mathrm{FSR}}$, where ω_{s} is the centre frequency of the signal field, corresponding to some mode of the OPO, and j is an integer.

According to (4), in the case of signal-photon generation on many cavity modes, the second-order correlation function between the signal and idler fields, $g^{(2)}_{\mathrm{s,i}}(\tau)$, consists of a series of peaks separated by the cavity round-trip time T_0, whose amplitude decays exponentially during the photon lifetime in the cavity [24]. The feasibility of observing the peaks depends on the relationship between the total resolution time of the detection apparatus [which is contributed by the temporal instability (jitter) of the electric pulse from the detector, the resolution time of the time-to-digital converter etc.] and the cavity round-trip time. In the limit of low resolution and short cavity length, the measured correlation function is described by an exponential decay:

$$g^{(2)}_{\mathrm{s,i}}(\tau) \propto \exp(-\Delta\omega_{\mathrm{mod}}\tau), \tag{5}$$

where τ is the time delay between the signal and idler photons. We obtain a similar result for generation in a single cavity mode, as would be expected.

3. Main results

Figure 1 shows a schematic of the experimental setup used for the generation and characterisation of SPDC-based narrow-band single-photon states. The nonlinear medium used was a periodically poled lithium niobate (PPLN) crystal doped with magnesium oxide, $LiNbO_3$:MgO (5%). The modulation period was $\Lambda = 7.47$ μm and the crystal length was 20 mm. The crystal was excited by a frequency-doubled cw neodymium laser at a wavelength of 532 nm, which caused photon pair generation in a type-0 (eee type) phase matching SPDC process at wavelengths of 867 and 1377 nm at a temperature of 85 °C.

The pump laser beam was focused into the nonlinear crystal by an $f = 200$ mm lens, so that the beam waist diameter was 70 μm. After traversing the crystal, the pump beam was suppressed by a cut-off filter F (70 dB attenuation at 532 nm) and dichroic mirror DM, which separated the signal and idler

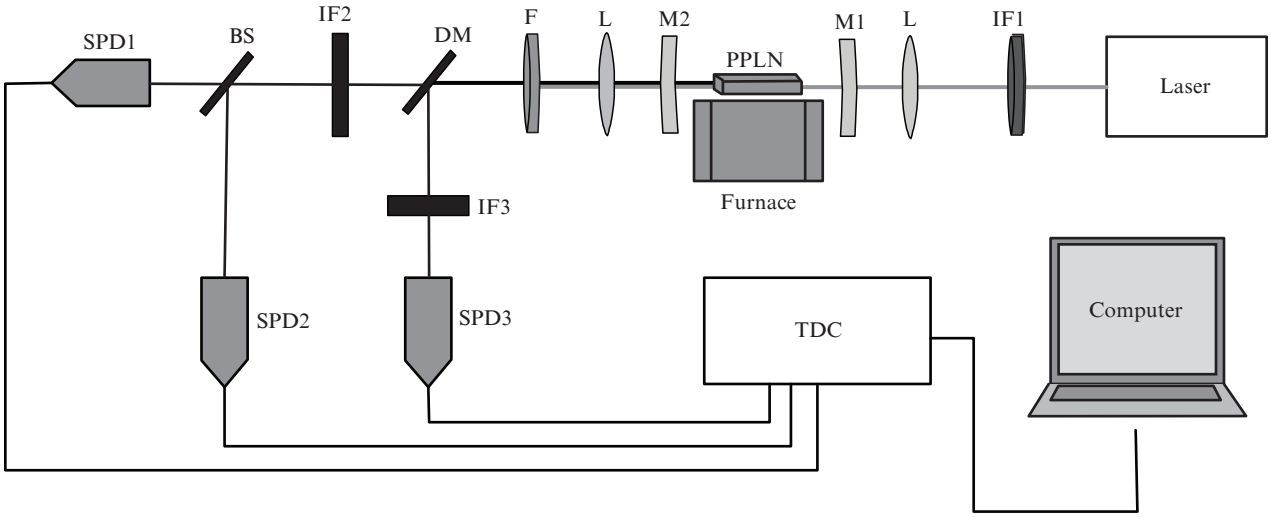

Figure 1. Schematic of the experimental setup used for SPDC-based generation of single-photon states:
(IF1) 532-nm interference filter; (L) $f = 200$ mm lenses; (M1, M2) cavity mirrors with reflectances $R_1 = 99.8\%$ and $R_2 = 97\%$ at a wavelength of 867 nm; (PPLN) periodically poled lithium niobate crystal; (F) 532-nm cut-off filter; (DM) 950-nm dichroic mirror; (IF2) 867-nm interference filter; (IF3) 1377-nm interference filter; (BS) 50/50 beam splitter; (SPD1, SPD2) visible single-photon detectors; (SPD3) infrared single-photon detector; (TDC) time-to-digital converter.

photons according to their wavelengths (867 and 1377 nm, respectively) into two channels. In each channel, the light was passed through interference filters IF2 and IF3 (867 and 1377 nm, respectively). The signal beam (867 nm) was divided by a beam splitter BS into two channels for second-order autocorrelation function $g^{(2)}(0)$ measurements in a Brown–Twiss interferometer configuration. It is worth noting that the autocorrelation function characterising the field of a single-photon source is measured and calculated with allowance for the heralding channel, so that it can be referred to as a conditional autocorrelation function [25]. In our case, the 1377-nm channel was used for heralding. Signal photons were detected by single-photon detectors SPD1 and SPD2 (SPCM-AQRH, PerkinElmer) in free-running mode with an efficiency $\eta_{867} = 40\%$, dark count rate of the order of 2 kHz and dead time of 150 ns. Idler photons were detected by detector SPD3 (ID201, ID Quantique) in free-running mode with an efficiency $\eta_{1377} = 10\%$, dark count rate of the order of 13 kHz and dead time of 14 μs.

The autocorrelation function $g^{(2)}(0)$ as a function of pump power was measured without mirrors M1 and M2. The measurement results are presented in Fig. 2. It is seen that there is a linear relation and that the contribution of multiphoton states increases with pump power. At pump powers much lower than 1 mW, the contribution of photodetector dark counts is significant and the relation is nonlinear. Nonlinearity is also observed at photodetector count rates near the saturation level.

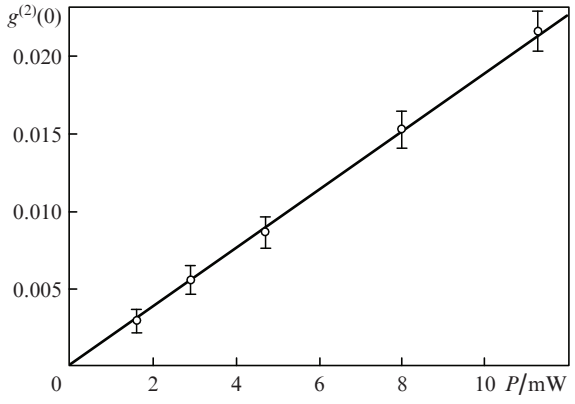

Figure 2. Zero-delay second-order autocorrelation function $g^{(2)}(0)$ as a function of pump power P.

To narrow down the parametric down-conversion spectrum, we used intracavity SPDC. The PPLN crystal was placed between mirrors M1 and M2, which had high transmission at the pump and idler wavelengths (532 and 1377 nm, respectively), so that the cavity amplified only the signal field at a wavelength of 867 nm, where mirrors M1 and M2 had reflectances $R_1 = 99.8\%$ and $R_2 = 97\%$, respectively, and the transmittance of the PPLN crystal was $T = 96.5\%$. At these parameters, the highest attainable finesse $\mathcal{F}$ was 26, the cavity mode bandwidth was 50 MHz, and the mode spacing was 1200 MHz.

Figure 3 shows measured $g^{(2)}_{s,i}(\tau)$ correlation functions. It is seen in Fig. 3a that the cavity round-trip time is comparable to the resolution time of the detection apparatus and that, in second-order correlation function measurements, we can detect only the envelope corresponding to the photon lifetime in the cavity. At a mirror separation of 10 cm (Fig. 3b), individual peaks begin to be resolved, which correspond to cavity mode locking and the spacing between which is determined by the cavity round-trip time. We carried out a number of experiments at different cavity lengths (from 8 to 15 cm) and, in each of them, obtained a perfect correspondence of the time spacing between the peaks in the correlation function with the cavity round-trip time. Moreover, fitting the correlation function envelope with the exponential decay (5) allowed us to determine the mode bandwidth and cavity finesse. A cavity length $l = 8$ cm corresponds to a mode bandwidth $\Delta\omega_{mod}/2\pi = 81.5$ MHz and finesse $\mathcal{F} = 18.5$. At $l = 10$ cm, we obtain $\Delta\omega_{mod}/2\pi = 73$ MHz and $\mathcal{F} = 20$. The photon pair generation rate in the crystal (with allowance for the optical loss in the channels) was 400 kHz at 1 mW of pump power.

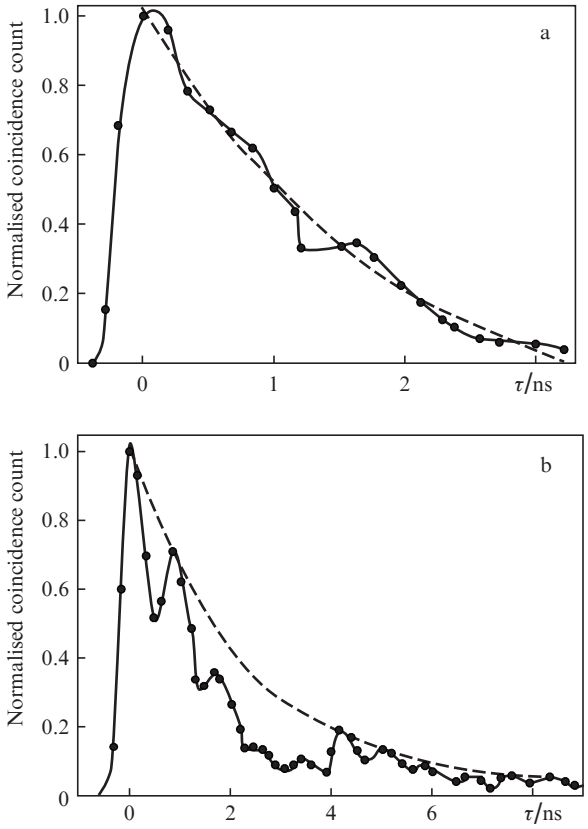

Figure 3. Coincidence counts between signal and idler photons as a function of the time delay between them at a cavity length l = (a) 8 and (b) 10 cm. The dashed lines represent fits of the correlation function envelope with an exponential decay.

4. Conclusions

We have experimentally demonstrated a narrow-band single-photon light source based on spontaneous parametric down-conversion in a single-resonant optical parametric oscillator. The linewidth of single-photon pulses emitted at a wavelength of 867 nm is as narrow is 70 MHz, which makes this source compatible with quantum memories based on a Nd^{3+}-doped isotopically pure Y^7LiF_4 crystal. The wavelength of the source can be tuned to an optical transition of the dopant ions by adjusting the temperature of the nonlinear crystal and the cavity mirror separation. In addition, the use of the single-

resonant optical parametric oscillator makes the source insensitive to pump wavelength fluctuations, significantly facilitating its operation.

Acknowledgements. This work was supported by the Russian Science Foundation (Grant No. 14-12-00806).

References

1. Kok P. *Contemp. Phys*., **57** (4), 526 (2016).
2. Reiserer A., Rempe G. *Rev. Mod. Phys*., **87** (4), 1379 (2015).
3. Walmsley I.A. *Science*, **348** (6234), 525 (2015).
4. Milburn G.J., Basiri-Esfahani S. *Proc. R. Soc. London, Ser. A*, **471** (2180), 20150208 (2015).
5. Eisaman M.D., Migdall J., Fan A., Polyakov S.V. *Rev. Sci. Instrum*., **82**, 071101 (2011).
6. Chunnilall C.J. et al. *Opt. Eng*., **53** (8), 081910 (2014).
7. Takeuchi S. *Jpn. J. Appl. Phys*., **53** (3), 030101 (2014).
8. Castelletto S.A., Scholten R.E. *Eur. Phys. J. Appl. Phys*., **41** (3), 181 (2008).
9. Klyshko D.N. *Sov. J. Quantum Electron*., **7** (5), 591 (1977) [*Kvantovaya Elektron*., **4** (5), 1056 (1977)].
10. Hong C.K., Mandel L. *Phys. Rev. Lett*., **56** (1), 58 (1986).
11. Ou Z.Y., Lu Y.J. *Phys. Rev. Lett.*, **83**, 2556 (1999).
12. Scholz M., Wolfgramm F., Herzog U., Benson O. *Appl. Phys. Lett*., **91**, 191104 (2007).
13. Nielsen B.M., Neergaard-Nielsen J.S., Polzik E.S. *Opt. Lett*., **34**, 3872 (2009).
14. Wolfgramm F., de Icaza Astiz Y.A., Beduini F.A., Cerè A., Mitchell M.W. *Phys. Rev. Lett*., **106**, 053602 (2011).
15. Fekete J., Rieländer D., Cristiani M., de Riedmatten H. *Phys. Rev. Lett*., **110** (22), 220502 (2013).
16. Förtsch M., Fürst J., Wittmann C., et al. *Nat. Commun*., **4**, 1818 (2013).
17. Luo K.-H., Herrmann H., Krapick S., et al. *New J. Phys.*, **17** (7), 073039 (2015).
18. Ahlrichs A., Benson O. *Appl. Phys. Lett*., **108** (2), 021111 (2016).
19. Rambach M., Nikolova A., Weinhold T., White A. *APL Photonics*, **1** (9), 096101 (2016).
20. Rieländer D., Lenhard A., Mazzera M., de Riedmatten H. *New J. Phys*., **18** (12), 123013 (2016).
21. Akhmedzhanov R. et al. *Phys. Rev. B*, **97** (24), 245123 (2018).
22. Belinsky A.V., Klyshko D.N. *Laser Phys.*, **4**, 663 (1994).
23. Mandel L., Wolf E. *Optical Coherence and Quantum Optics* (New York: Cambridge University Press, 1995).
24. Herzog U., Scholz M., Benson O. *Phys. Rev. A*, **77**, 023826 (2008).
25. Beck M. *J. Opt. Soc. Am. B*, **24** (12), 2972 (2007).